ACS Chemical Neuroscience

ARTICLE

pubs.acs.org/acschemicalneuroscience

A Safe, Blood-Brain Barrier Permeable Triphenylmethane Dye Inhibits Amyloid-β Neurotoxicity by Generating Nontoxic Aggregates

H. Edward Wong,[†] Wei Qi,[†] Hyung-Min Choi,[†,§] Erik J. Fernandez,[†] and Inchan Kwon[*,†,‡]

[†]Department of Chemical Engineering and [‡]Institute on Aging, University of Virginia, Charlottesville, Virginia 22911, United States

[§]Department of Organic Materials and Fiber Engineering, Soongsil University, Seoul, Republic of Korea 156-743

Supporting Information

ABSTRACT: Growing evidence suggests that on-pathway amyloid-β (Aβ) oligomers are primary neurotoxic species and have a direct correlation with the onset of Alzheimer's disease (AD). One promising therapeutic strategy to block AD progression is to reduce the levels of these neurotoxic Aβ species using small molecules. While several compounds have been shown to modulate Aβ aggregation, compounds with such activity combined with safety and high blood-brain barrier (BBB) permeability have yet to be reported. Brilliant Blue G (BBG) is a close structural analogue of a U.S. Food and Drug Administration (FDA)-approved food dye and has recently garnered prominent attention as a potential drug to treat spinal cord injury due to its neuroprotective effects along with BBB permeability and high degree of safety. In this work, we demonstrate that BBG is an effective Aβ aggregation modulator, which reduces Aβ-associated cytotoxicity in a dose-dependent manner by promoting the formation of off-pathway, nontoxic aggregates. Comparative studies of BBG and three structural analogues, Brilliant Blue R (BBR), Brilliant Blue FCF (BBF), and Fast Green FCF (FGF), revealed that BBG is most effective, BBR is moderately effective, and BBF and FGF are least effective in modulating Aβ aggregation and cytotoxicity. Therefore, the two additional methyl groups of BBG and other structural differences between the congeners are important in the interaction of BBG with Aβ leading to formation of nontoxic Aβ aggregates. Our findings support the hypothesis that generating nontoxic aggregates using small molecule modulators is an effective strategy for reducing Aβ cytotoxicity. Furthermore, key structural features of BBG identified through structure–function studies can open new avenues into therapeutic design for combating AD.

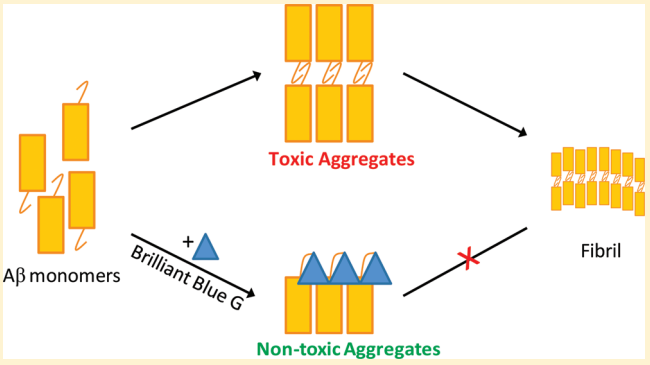

KEYWORDS: Alzheimer's disease, amyloid-β, oligomers, Brilliant blue, nontoxic aggregates, fibrils

With an ever increasing number of new cases each year, Alzheimer's disease (AD) has become the most common form of senile dementia. The disease is primarily diagnosed in persons over the age of 65.[1] Symptoms manifest in a slow and progressive manner, but are ultimately debilitating and fatal. Currently, 5.3 million people in the United States are affected by AD, with the number projected to rise to 13.5 million by 2050.[2] Although several United States Food and Drug Administration (FDA)-approved drugs temporarily reduce symptoms, no treatment exists that slows or stops the progression of AD.

A pathological hallmark of AD is the accumulation of insoluble protein aggregates, composed primarily of neurotoxic amyloid-β (Aβ). Aβ is created from sequential proteolytic cleavage of the amyloid precursor protein (APP) by the β- and γ-secretases.[3] Although a number of Aβ isoforms, with lengths from 39 to 43 residues, are generated, Aβ40 and Aβ42 are the most physiologically relevant. In AD patients, Aβ40 and Aβ42 are found in an approximate 9:1 ratio, but Aβ42 is more aggregation-prone.[4]

According to the original amyloid-cascade hypothesis, conversion of soluble Aβ monomers into insoluble fibrils causes AD onset.[5] Recently, this hypothesis has been further refined. Growing evidence suggests that certain types of soluble Aβ oligomers and protofibrils are more toxic than Aβ fibrils, and their presence correlates strongly with dementia.[6−9] Therefore, reduction of neurotoxic Aβ oligomers and protofibrils represents a promising strategy to inhibit Aβ-associated neurotoxicity.

Numerous small molecules have been studied for their ability to modulate Aβ aggregation and reduce neurotoxicity.[10−13] Congo red, an amyloid-structure specific dye, has the ability to modulate fibril formation and reduce Aβ neurotoxicity.[14−18] Besides amyloid-specific dyes, several lipid-based modulators and polyphenols, such as scyllo-inocitol, nordihydroguaiaretic acid, curcumin, epigallocatechin gallate (EGCG), and resveratrol, have been reported to modulate Aβ aggregation and reduce Aβ-associated toxicity.[10,19−25] Although the results from these molecules are encouraging and validate Aβ aggregation modulation

Received: June 12, 2011
Accepted: September 6, 2011
Published: September 06, 2011

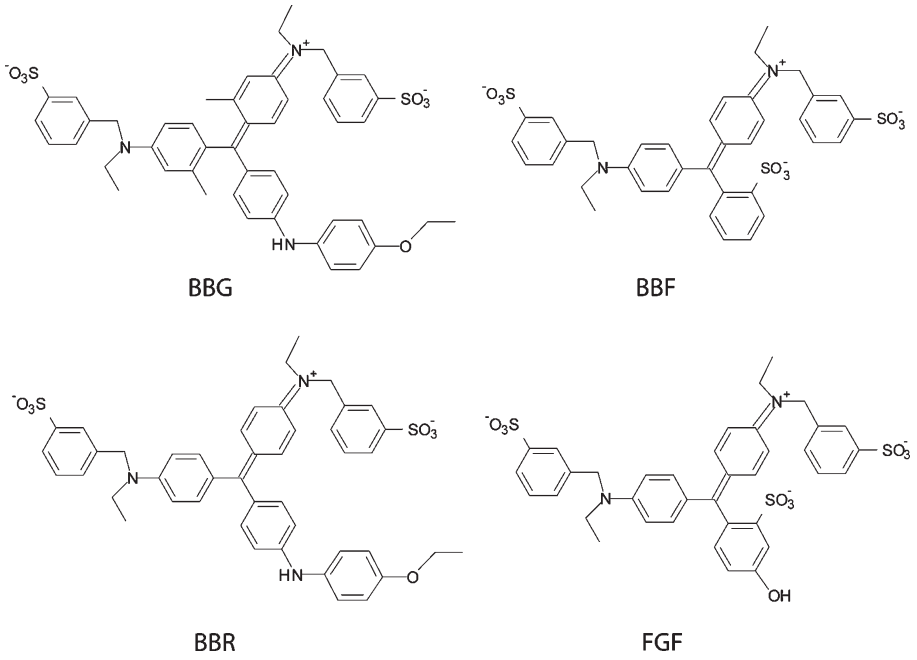

Figure 1. Chemical structures of Brilliant Blue G (BBG), Brilliant Blue FCF (BBF), Brilliant Blue R (BBR), and Fast Green FCF (FGF) at neutral pH.

as a promising strategy, a practical and effective therapeutic has yet to be identified. Most Aβ aggregation small-molecule modulators identified are not suitable for AD therapeutic leads because they lack low toxicity or blood-brain barrier (BBB) permeability. Crossing the blood-brain barrier is a big challenge in AD drug development; 98% of small molecule drugs and almost 100% of large molecule drugs cannot cross the BBB.[26] For example, therapeutic application of Congo red has been hindered by poor BBB permeability as well as carcinogenicity.[27] Although several polyphenol-based Aβ modulators including tannic acid and EGCG are very effective in reducing Aβ neurotoxicity in cell-based assays,[21,28] tannic acid and EGCG does not cross the animal BBB and the human BBB, respectively.[29−31] As a result, there remains a strong driving force to identify new small-molecule AD therapeutic candidates that modulate Aβ aggregation and are also safe and BBB-permeable.

In this Article, we identify a new Aβ modulator with all of these properties. To our knowledge, Aβ modulating capacities of triphenylmethane dyes have not yet been reported. Here we show that Brilliant Blue G (BBG), a triphenylmethane dye (Figure 1) with a demonstrated safety profile[32] and BBB-permeability,[33] also substantially removes Aβ cytotoxicity even at below stoichiometric concentrations. Brilliant Blue FCF (BBF), a close structural analogue of BBG, is approved by the FDA as a blue food dye (Figure 1) and has one of the highest safety profiles among the seven currently approved synthetic food dyes. In tests, it exhibits no observable toxicity up to a daily consumption of 600 mg/kg body mass in healthy animals.[34] In the United States, more than six thousand pounds of BBF is produced annually, and daily intake of up to 12.5 mg/kg is tolerable in humans.[35] BBG has recently garnered prominent attention in neuroscience regarding its therapeutic potential to treat acute spinal cord injury. In animal models, systemic administration of BBG reduced damage and expedited recovery after spinal cord injury.[33] BBG also confers neuroprotection to the brain by inhibiting adverse inflammatory reactions and mitigates multiple sclerosis symptoms.[36,37] With the possibility for systemic administration into the nervous system with no known adverse side effects, BBG is an attractive Aβ aggregation modulator candidate.

In this Article, we explore BBG's ability to modulate Aβ aggregation and reduce neurotoxicity with biochemical, biophysical, and cell-based assays. In particular, we monitored Aβ oligomer formation via immunoblotting using Aβ-conformation specific antibody, A11. Polyclonal A11 antibody reacts with Aβ oligomers and protofibrils, including neurotoxic conformers, but not with Aβ monomers and fibrils.[8,38,39] We report that BBG promotes Aβ monomer conversions into nontoxic aggregates. To begin identifying the BBG structural features responsible for this activity, we also evaluated the modulating capacities of three close structural analogues, Brilliant Blue R (BBR), BBF, and Fast Green FCF (FGF) on Aβ aggregation and cytotoxicity. Our findings suggest that the structural differences of BBG and BBR from BBF and FGF along with the two additional methyl groups attached to the triphenylmethane structure of BBG are important for effective modulation of Aβ aggregation and cytotoxicity. Unique interaction modes of BBG and BBR with Aβ are expected to provide new insight on molecular mechanism of Aβ aggregation and cytotoxicity. Our findings validate a relatively new hypothesis that generating nontoxic Aβ aggregates by small molecules is an effective way to reduce Aβ-associated neurotoxicity even without preventing Aβ oligomer formation.[21,28] Thus, our work provides evidence of and mechanistic details of reduced Aβ-associated neurotoxicity for a novel type of Aβ aggregation modulator that also has encouraging attributes as a therapeutic lead compound.

RESULTS AND DISCUSSION

Modulation of Aβ Aggregation by BBG. In order to evaluate the aggregation modulating capability of BBG, we employed dot-blotting, transmission electron microscopy (TEM), and the thioflavin T (ThT) fluorescence assay. TEM and ThT fluorescence assays are widely used to monitor Aβ aggregation. TEM images

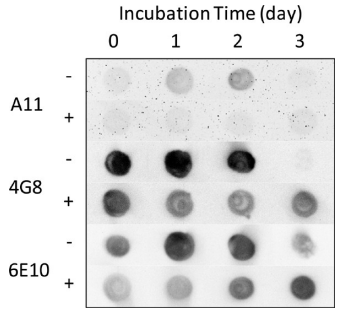

Figure 2. Monitoring Aβ aggregation by dot-blotting. Oligomer-specific A11 antibody and Aβ-sequence specific antibodies, 4G8 and 6E10, were used. 50 μM Aβ was incubated in the absence (−) (top panels) or presence of 3× BBG (+) (bottom panels) for 1−3 days at 37 °C. Samples were taken on the indicated day and spotted onto a nitrocellulose membrane. Each membrane was immunostained with the A11, 4G8, or 6E10 antibody. The blot images were taken using a UVP BioSpectrum imaging system.

provide morphological information of Aβ aggregates. ThT is a dye that fluoresces at 485 nm when it binds to amyloid fibrils.[23,40,41] Therefore, ThT fluorescence measurement is an efficient tool to monitor the progression of fibril formation. However, the ThT assay is not very effective in detecting soluble oligomers that are known to be more neurotoxic than amyloid fibrils.[6−9] Furthermore, the diversity of Aβ aggregate morphologies and differing levels of neurotoxicity[42,43] represent a challenge for correlating the aggregate morphology observed by TEM to Aβ-associated neurotoxicity. Recently, dot-blotting with Aβ-specific antibodies was successfully used to detect and distinguish the spectrum of Aβ conformer species.[8,38,39,44−46] In particular, A11 is useful for detecting neurotoxic Aβ intermediates.[39,45] Previously it was shown that Aβ-associated toxicity could be mitigated by reducing the presence of A11-reactive species.[8,21] Alternatively, 4G8 is an Aβ-sequence-specific monoclonal antibody[47−50] which has an epitope that lies within amino acids 17−24 of Aβ. The 4G8 epitope corresponds to a region of the Aβ peptide that is known to form β-sheet structures. During transition from monomers and low molecular weight oligomers to fibrils, β-sheet stacking buries the 4G8 epitope and ultimately limits 4G8 antibody binding. This leads to a dramatic loss of the 4G8 signal which can thereby be used to detect extensive fibril network structure formation.[51] Lastly, 6E10 is a monoclonal antibody that recognizes residues 1−16 of Aβ, the N-terminus of Aβ.[45,51] Although the 6E10 antibody was originally thought to bind various Aβ species with equal strength, recent studies indicate that the 6E10 antibody binds to different Aβ species with different binding affinities.[13,45,52] Similar to the 4G8 antibody, the 6E10 antibody binding affinity to fibrils is a few times lower than those of oligomers and monomers. According to the structural model of Aβ40 fibril proposed by Grigorieff et al., two pairs of Aβ protofibrils intertwine adjacently to form a fibril.[53] In their model, the N-terminus of the each protofibril is interlocked to form a fibril, which can bury the 6E10 epitope upon fibril formation. We performed dot-blotting using a panel of Aβ-specific antibodies, together with traditional TEM and ThT fluorescence assay, to monitor the formation of neurotoxic Aβ oligomers, protofibrils, and fibrils.

Two pathologically important Aβ isoforms, Aβ42 and Aβ40, have been widely used to evaluate the modulating capacities of numerous small molecules on Aβ aggregation and cytotoxicity.[54−58] We used the more abundant isoform, Aβ40, in this study. Aβ samples were prepared by incubating 50 μM of Aβ40 monomer from 0 to 3 days at 37 °C without shaking in either the absence (control) or presence of BBG as described previously.[59−61] In order to detect even a weak modulating effect of BBG on Aβ aggregation, we chose 150 μM of BBG (3× BBG), which is 3 times higher than the concentration of Aβ (50 μM). Aβ samples were taken periodically during incubation and subjected to dot-blotting, the ThT fluorescence assay, and TEM.

In the absence of BBG, dot-blotting results indicated that the majority of A11-reactive Aβ aggregates formed between day 1 and 2 (Figure 2). However, when the Aβ monomer was coincubated with BBG, A11-reactivities signals remained very low until day 3. However, reduction of the A11-reactivities signals at day 1 and 2 did not result from a loss of Aβ moieties, as supported by the sustained 6E10 signal at days 1 and 2 compared to day 0 (Figure 2). In the absence of BBG, the 6E10 signal was highest at days 1 and 2 and then decreased at day 3 (Figure 2). This variation can be explained by the weaker binding affinity of 6E10 for Aβ monomers and fibrils compared to Aβ intermediates as described previously.[52] In the presence of 3× BBG, the 6E10 signal at day 3 was very strong, suggesting the idea that Aβ intermediates rather than Aβ fibrils were predominant in the sample. In the Aβ control sample, the majority of 4G8 signal was lost between day 2 and 3 (Figure 2), implying that the majority of 4G8 epitopes were buried due to compact stacking of β-sheet structures, a prototypical feature of amyloid fibrils.[51] However, in the presence of 3× BBG, a significant 4G8 signal at day 3 was observed, which also supports the idea that Aβ fibril mesh networks were not formed. These findings imply that BBG effectively inhibits the formation of A11-reactive Aβ oligomers and Aβ fibrils, the most toxic Aβ species.

Next we characterized the morphology of the Aβ species formed with and without BBG using negative-stain TEM. TEM images clearly show a distinct morphological difference between Aβ samples incubated in the absence and those in the presence of 3× BBG (Figure 3). At day 1, in the absence of BBG, oligomers and protofibrils (∼100 nm in length) were formed (Figure 3, top-left). Considering that high molecular weight Aβ protofibrils as well as oligomers were A11-reactive in the literature,[21,39,62] there is the possibility that the protofibrils observed at day 1 were also A11-reactive. Interestingly, even in the presence of 3× BBG, protofibrils (∼100 nm in length) were predominantly observed (Figure 3, bottom-left panel). Despite the morphological similarities, the Aβ aggregates prepared with 3× BBG possessed substantially lower immunoreactivity to the A11 antibody than those prepared without BBG. These findings imply that, at day 1, the low A11 reactivity of Aβ samples coincubated with BBG resulted from promoted formation of A11-unreactive Aβ protofibrils.

At day 2, a mixture of protofibrils and fibrils was observed in the absence of BBG (Figure 3, top-middle; Figure 4A), which indicated that some Aβ oligomers and protofibrils were converted into longer protofibrils and fibrils. However, in the presence of 3× BBG, protofibrils (less than 100 nm) were still predominantly observed similar to day 1 (Figure 3, bottom-middle).

At day 3, the Aβ sample prepared in the absence of BBG exhibited only long mature fibrils in a meshed network (Figure 3, top-right), which is consistent with dot-blotting and ThT fluorescence results. Here, ThT fluorescence sharply increased beginning at 48 h (Figure 5), which was interpreted to be the

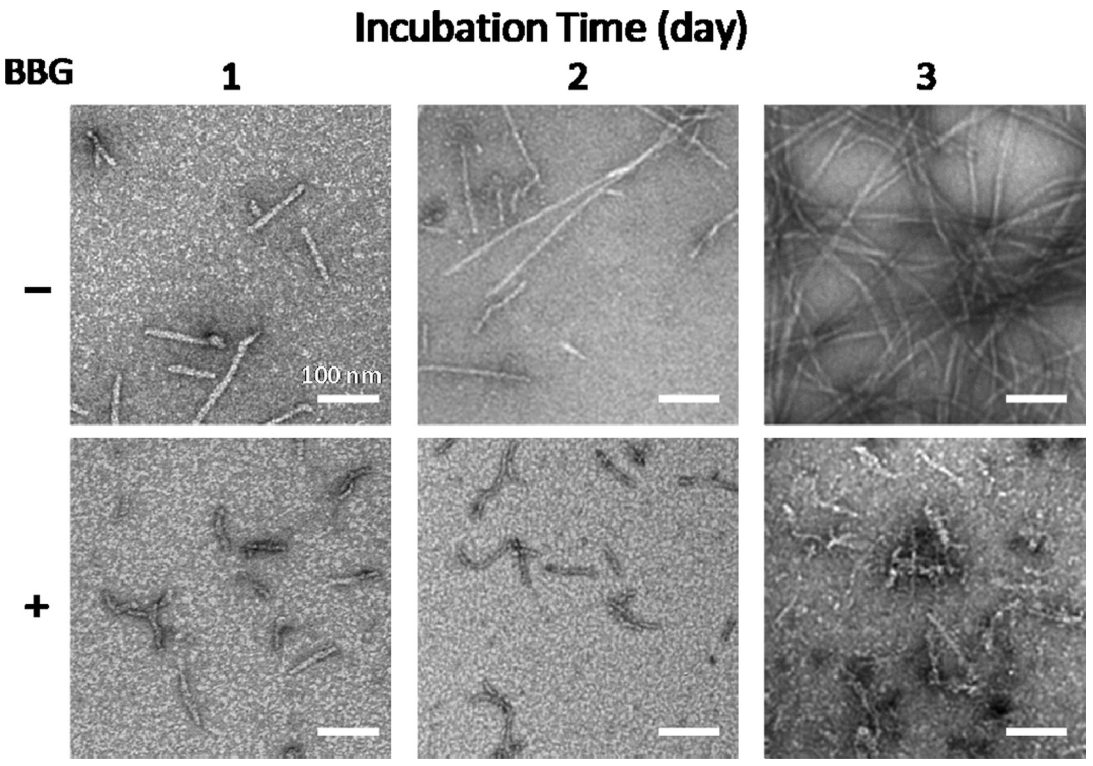

Figure 3. Monitoring Aβ aggregate and fibril formation by TEM. 50 μM Aβ was incubated in the absence (−) (top panels) or presence of 3× BBG (+) (bottom panels) for 1−3 days at 37 °C. Presence of oligomers and protofibrils (top-left); protofibrils and isolated fibrils (top-middle); fibril mesh network (top-right); oligomers and protofibrils (bottom-left); protofibrils (bottom-middle); protofibrils (bottom-right). Scale bar is 100 nm.

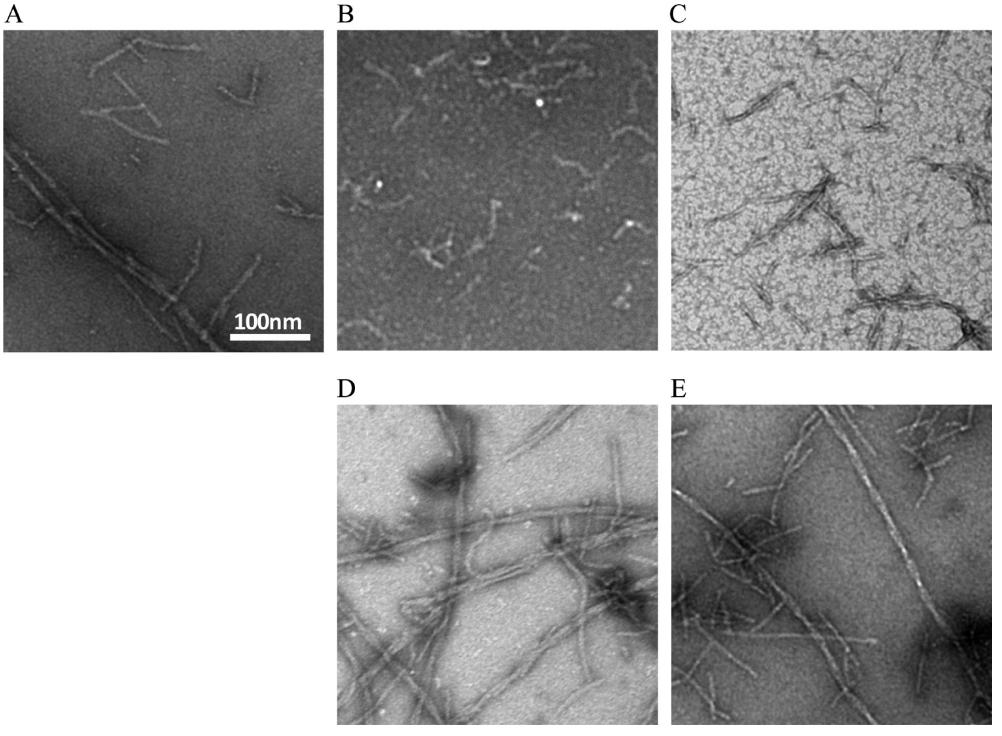

Figure 4. TEM images of 50 μM of Aβ incubated for 2 days at 37 °C in the absence of any dye (A), or in the presence of 10× BBG (B), 10× BBR (C), 10× BBF (D), or 10× FGF (E). Scale bar is 100 nm.

onset of amyloid fibril formation. In dramatic contrast, in the presence of 3× BBG, TEM showed that protofibrils (∼100 nm) remained the predominant species (Figure 3, bottom-right), which supports the idea that coincubation of 3× BBG stops or

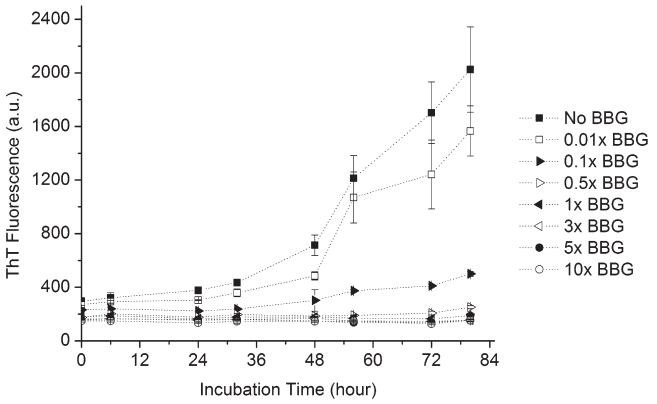

Figure 5. Time course of ThT fluorescence of Aβ samples with varying concentrations of BBG. 50 μM of Aβ monomer was incubated at 37 °C in the absence (no BBG) or presence of the indicated concentrations of BBG (from 0.001× to 10×) for up to 80 h. 5 μL of Aβ sample was taken at 0, 6, 24, 32, 48, 54, 72, and 80 h for ThT fluorescence analysis. ThT fluorescence was measured in arbitrary units (a.u.). Values represent means ± standard deviation (n = 3).

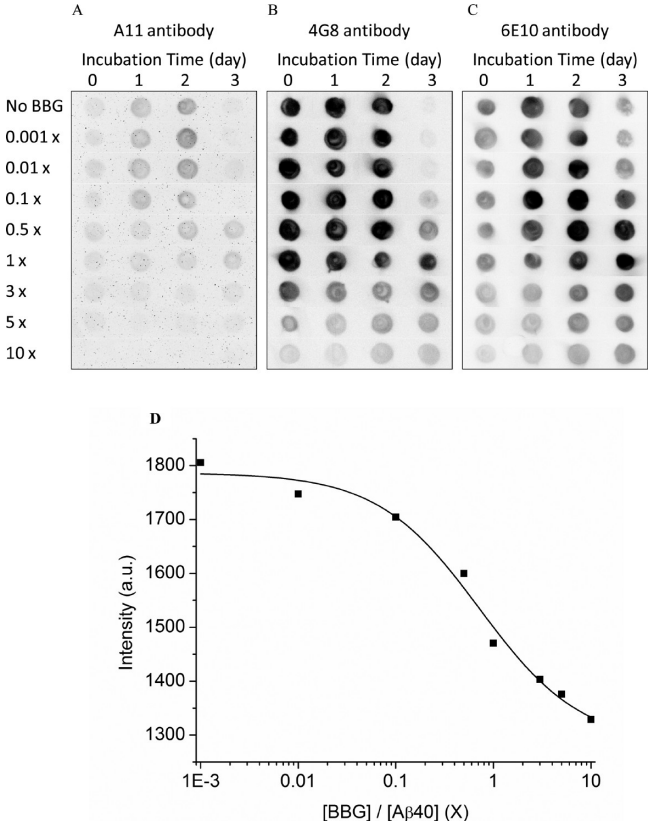

Figure 6. Dose-dependence of Aβ aggregation modulation by BBG. 50 μM of Aβ monomer was incubated at 37 °C in the absence (no BBG) or presence of the indicated concentrations of BBG (from 0.001× to 10×) for up to 3 days. Samples were taken on the indicated day and spotted onto a nitrocellulose membrane. Each membrane was immunostained with the A11 (A), 4G8 (B), or 6E10 (C) antibody. The blot images were taken using a UVP BioSpectrum imaging system. The blot image of the A11-reactive signal of Aβ samples incubated with varying concentrations of BBG for 2 days was processed by ImageJ (NIH). The data were fitted to a sigmoid curve (R^2 = 0.99) (D).

at least substantially slows down the Aβ aggregation process. Morphological similarities among the BBG-treated Aβ aggregates

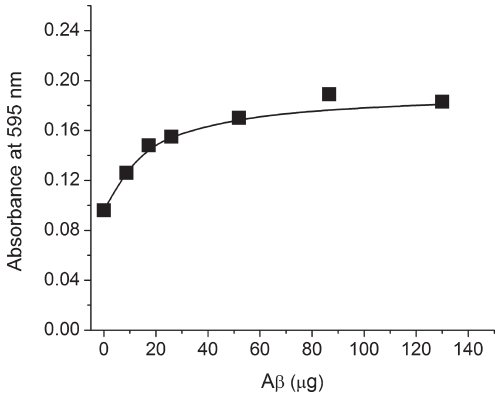

Figure 7. Saturation binding curve of BBG into Aβ peptide. 49 μM BBG was incubated with varying concentrations of Aβ peptide (0–300 μM) until equilibrium was reached and the absorbance of the BBG bound to the Aβ peptide was measured at 595 nm.

observed at days 1, 2, and 3 are consistent with very weak A11-reactivity of the BBG-treated samples at least until day 3.

Thse findings support that BBG is an efficient aggregation modulator and reduces the formation of A11-reactive Aβ aggregates. The results also show that BBG suppresses fibril formation for at least 3 days.

Dose-Dependent Modulation of Aβ Aggregation by BBG. To further characterize the aggregation modulation capabilities of BBG, we evaluated BBG dose-dependent aggregation using dot-blotting and the ThT fluorescence assay. Aβ (50 μM) was coincubated at 37 °C with various BBG concentrations ranging from 0.001× (50 nM) to 10× (500 μM). Dot-blotting results of Aβ samples using three Aβ-specific antibodies (A11, 4G8, and 6E10) are shown in Figure 6. When Aβ was coincubated with less than 0.1× BBG (5 μM), no observable changes were found in the A11 immunoblotting patterns (Figure 6A). However, coincubation with 0.5× BBG or greater resulted in a reduction in the concentration of A11-reactive species formed, over the course of the study, confirming previous results. Since A11-reactive Aβ species were most abundant at day 2, we wanted to quantify the inhibition of A11-reactive Aβ species formation (Figure 6D). Therefore, for day 2, integrated A11 dot-blot signal intensities were plotted against BBG concentrations. A half-maximal inhibitory concentration (IC_{50}) of 0.72× BBG was derived from the data fitting to a sigmoid curve (R^2 = 0.99).

In the absence of BBG, the 6E10 antibody stained Aβ oligomers/protofibrils, monomers, and fibrils in decreasing order of intensity, which is consistent with a few fold weaker binding to Aβ fibrils by the 6E10 compared to oligomers/protofibrils as described previously.[52] In Figure 6B and C, below 1× BBG concentrations, 4G8 and 6E10 signals increase at day 3. These results are consistent with enhanced accessibility of the 4G8 and 6E10 epitopes due to BBG-induced conversion of Aβ aggregates from fibril mesh networks to oligomers and protofibrils. However, as the concentration of BBG increased above 1×, 4G8 and 6E10 reactive signals decreased. Finally, in the presence of 10× BBG, the 4G8- and 6E10-reactive signals are both very weak compared to those observed in the absence of BBG, suggesting that both 4G8 and 6E10 epitopes were substantially lost partially due to direct binding of BBG. The 4G8 epitope corresponds to a hydrophobic patch of the Aβ that is known to form β-sheet structures. The 6E10 epitope is the N-terminus of Aβ carrying

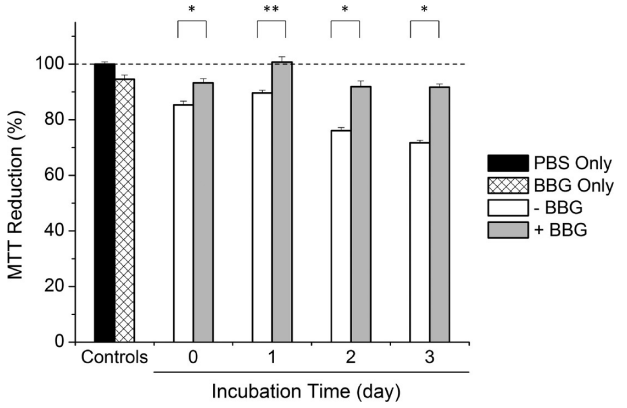

Figure 8. Viability of neuroblastoma SH-SY5Y cells incubated with preformed Aβ samples in the absence or presence of BBG. Preformed Aβ aggregates were prepared by incubating 50 μM of Aβ monomer in the absence or presence of BBG at 37 °C for 0−3 days, as indicated in the graph. Aggregates were then administered to SH-SY5Y cells at a final concentration of 5 μM. After 48 h, mitochondrial metabolic activity was measured using MTT reduction. Cells administered with PBS as a control (black), 3× BBG (15 μM) dye only (white with pattern), Aβ incubated without BBG (white), and Aβ incubated with 3× BBG (gray). Values represent means ± standard deviation ($n \geq 3$). Values are normalized to the viability of cells administered with PBS only. Two-sided Student's *t* tests were applied to the data. *$P < 0.001$, **$P < 0.005$.

both positive and negative charges. Therefore, we speculate that BBG preferentially binds to the hydrophobic patch of Aβ and weakly binds to the charged N-terminus of Aβ via electrostatic interaction.

BBG Binding to Aβ. Immunoblotting assays described in the previous section suggested that BBG binds to multiple sites on Aβ above 1× BBG concentration. In order to determine the number of BBG binding sites on Aβ, a binding curve (Figure 7) was obtained according to the method described previously.[63] The number of binding sites (n) and the intrinsic association constant (k), 3.2 and 1.1 × 10^4 (M^{-1}), respectively, were determined by fitting the BBG-Aβ binding data to a straight line in the double reciprocal plot (Supporting Information Figure S1) in the Supporting Information Section. Multiple BBG binding site on Aβ can explain the reduced 4G8 and 6E10 reactivities of Aβ aggregates at high concentrations of BBG considering the reduced accessibility of the 4G8 and 6E10 antibodies to their epitopes caused by BBG binding. The dissociation constant, the reciprocal of the intrinsic association constant, is 92 μM.

Inhibition of Aβ-Associated Cytotoxicity by BBG. Next, we sought to determine whether the conversion of A11-reactive aggregates into off-pathway aggregates reduces Aβ-associated neurotoxicity. In order to evaluate the cytotoxicity of Aβ species, we employed the 3-(4,5-dimethylthiazol-2-yl)-2,5-diphenyltetrazolium bromide (MTT)-reduction assay and neuroblastoma SH-SY5Y cells, widely used for this purpose.[8,22,64−69] Although the MTT-reduction assay does not directly measure cell death, it detects a change in cellular redox activity that is considered an indication of cell viability.[70] Therefore, inhibition of MTT reducing activity of cells has been often interpreted as cytotoxicity. Preformed Aβ aggregates were prepared by incubating Aβ monomers in the absence or presence of 3× BBG at 37 °C for the specified time duration. The preformed aggregates were then administered to neuroblastoma SH-SY5Y cells for 48 h, and subsequently cell viability was measured by MTT reduction. Before testing the cytotoxicity of Aβ samples, we first determined whether BBG by itself is cytotoxic to neuroblastoma SH-SY5Y cells. In the presence of 3× BBG dye (15 μM), SH-SY5Y cell viability was 95% of that in the absence of any BBG, which is quite consistent with the good biocompatibility and low toxicity observed in animals.[32,33]

Next we evaluated Aβ-associated toxicity. At day 0, cells treated with Aβ monomers (5 μM) exhibited a mild reduction (15%) in the viability (Figure 8), which may be due to moderately toxic Aβ aggregates formed during the 48 h incubation of Aβ monomers with the cells. In the presence of 3× BBG (15 μM), viability recovered to 93% ($P < 0.001$), which is similar to the viability of cells treated with 3× BBG dye alone without Aβ monomer (95%). This finding suggests that 3× BBG inhibits toxic aggregate formation from Aβ monomers (5 μM) during the 48 h incubation with the cells. At day 1, in the presence of 3× BBG, the Aβ sample exhibited cell viability of 101%, significantly higher than the cell viability (90%) of Aβ samples without BBG ($P < 0.001$) (Figure 8). These findings support the hypothesis that BBG can counteract the Aβ sample cytotoxicity and that BBG-induced Aβ aggregates observed by TEM were nontoxic.

At day 2, in the absence of BBG, cell viability decreased to 76%. This can likely be attributed to an increased concentration of A11-reactive toxic intermediates and to the emergence of amyloid fibrils (Figure 8). Although amyloid fibrils are less toxic than A11-reactive toxic intermediates, the toxicity of amyloid fibrils is reportedly higher than that of monomers.[8,9] In the presence of BBG, cell viability significantly improved to 92% ($P < 0.001$), consistent with the reduction of A11-reactive Aβ species in the dot-blot results (Figure 2) and lack of observable fibrils in the TEM image (Figure 3). These results suggest that a decrease in the concentration of A11-reactive species correlates with a decrease in Aβ-associated toxicity.

At day 3, in the absence of BBG, addition of the preformed Aβ aggregates reduced the cell viability to 72%. Although the A11-reactivity dropped after day 2, the reduced viability was most probably caused by the predominant amyloid fibrils converted from both small fraction of toxic A11-reactive aggregates and probably more dominant non-A11 reactive large intermediates. Ishii and co-workers showed that Aβ aggregates larger than 50 kDa were 5 times less toxic than Aβ aggregates smaller than 50 kDa.[9] Based on dot-blotting, TEM and fluorescence, the vast majority of fibrils were formed almost exclusively after day 2 (Figures 2, 3, and 5). Consequently, at day 3, fibrils were the major toxic moieties. However, when Aβ was incubated with 3× BBG, cell viability was significantly recovered to 92% ($P < 0.001$), which is comparable to the viability of cells incubated only with 3× BBG, without Aβ. Based on the cell viability results, we conclude that 3× BBG completely mitigates Aβ-associated cytotoxicity. Moreover, these findings suggest that the majority of oligomers and protofibrils formed in the presence of 3× BBG observed in TEM in fact are nontoxic and structurally distinct from toxic Aβ species formed in the absence of BBG. This confirms that BBG reduces Aβ-associated toxicity by promoting the conversion of Aβ monomer to off-pathway, nontoxic intermediates.

Although an MTT reduction assay has been widely used to determine Aβ-associated cytotoxicity on numerous cell lines,[21,45,71−75] the MTT reduction assay results should be carefully interpreted due to a potential issue of Aβ-induced expedited exocytosis of the reduced MTT. There have been several reports indicating that Aβ aggregates can increase export of the reduced MTT and promote buildup of the crystalline form of the reduced MTT on the cell surface, leading to a reduced

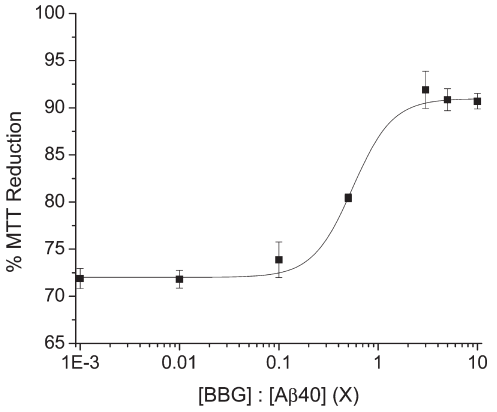

Figure 9. Dose-dependence of inhibition of Aβ-associated cytotoxicity by BBG. Preformed Aβ aggregates were prepared by incubating 50 μM of Aβ monomer in the presence of varying concentrations of BBG (0.001×, 0.01×, 0.1×, 0.5×, 1×, 3×, 5×, and 10×) at 37 °C for 2 days. Aβ aggregates were then administered to SH-SY5Y cells at a final concentration of 5 μM. After incubation, mitochondrial metabolic activity was measured after 48 h using MTT reduction. Values represent means ± standard deviation ($n \geq 3$). Values are normalized to the viability of cells administered with PBS only. The data were fitted to a sigmoid curve ($R^2 = 0.99$).

MTT uptake.[76−78] Considering other researchers have reported a good correlation between a MTT reduction and other viability assay results, including oxidative stress[73] and lactate dehydrogenase (LDH) release,[75] the increased MTT exocytosis may be dependent on the cell type and Aβ preparation method used.

In order to confirm the correlation of the MTT assay results with Aβ-associated cytotoxicity, an alamar blue reduction assay was also performed. Alamar blue reducing cellular activity has been considered an indication of cell viability and used to measure Aβ-associated cytotoxicity.[79−81] Since alamar blue is a soluble dye, it does not cause an issue of crystal dye buildup on the cell surface. Aβ samples incubated for 0−3 days at 37 °C were added to SH-SY5Y cells to determine alamar blue reducing activities. Similar to the MTT reduction assay results, the cells treated with Aβ aggregates incubated for 2 days exhibited significantly ($P < 0.05$) lowered alamar blue reducing activity compared to the cells without Aβ treatment (control) or cells treated with Aβ monomers (day 0) (Supporting Information Figure S2). Furthermore, coincubation of 3× BBG with Aβ for 2 days inhibited the Aβ-induced loss of the alamar blue reducing activity ($P < 0.05$) (Supporting Information Figure S2), which is also consistent with the MTT reduction assay results. However, there were two factors making it difficult to detect a subtle change in the alamar blue reducing activity under the other conditions used in our studies. First, the differences in the alamar blue reducing cellular activities with different Aβ samples were smaller than those in the MTT reducing activities at similar conditions. Second, the standard deviations of the measured alamar blue reducing activities (5−11%) were greater than those in the MTT reducing activities (usually less than 5%). Despite the limitations, the alamar blue assay results support the idea that the decrease in the MTT reducing activity of cells treated with Aβ aggregates (at least at day 2) indicates the Aβ-associated cytotoxicity and the recovery of MTT reducing activity in the presence of 3× BBG means a reduction of the Aβ-associated cytotoxicity under the conditions used in our studies. Therefore, we believe that the MTT reduction assay results have a good correlation with the cell viabilities treated with the Aβ samples, though we do not completely exclude the possibility that the promoted crystal buildup of the reduced MTT contributes to the MTT reduction results.

Dose-Dependent Inhibition of Aβ-Associated Cytotoxicity by BBG. In order to evaluate the ability of BBG to inhibit Aβ-associated cytotoxicity at varying doses, preformed Aβ aggregates were prepared by incubating Aβ monomer in the absence (control) or presence of varying concentrations of BBG from 0.001× to 10× at 37 °C for 2 days. The resulting preformed species were administered to SH-SY5Y cells, and viability was measured after 48 h using MTT reduction. From 0.001× (5.0 nM) to 0.1× (0.5 μM) BBG, cell viability (approximately 72%) was comparable to that of the control. However, cell viability dramatically improved when 0.5× BBG (2.5 μM) or greater was coincubated with Aβ (Figure 9). Consequently, from 3× to 10× BBG, cell viability was maintained in the range of 91 to 93%. When the data were fitted to a sigmoid dose-dependent curve ($R^2 = 0.99$), a half maximal effective concentration (EC_{50}) value of 0.55× BBG was obtained. This value corresponded almost exactly to the significant reduction in the Aβ-associated cytotoxicity observed at 0.5× BBG. These results clearly demonstrate that BBG inhibits Aβ-associated cytotoxicity in a dose-dependent manner.

Based on the results described earlier, it is obvious that BBG inhibits formation of A11-reactive Aβ species and Aβ-associated cytotoxicity in a dose-dependent manner. Furthermore, the EC_{50} value (0.55× BBG) derived from Aβ-associated cytotoxicity sigmoidal regression (Figure 9) corresponds well to the IC_{50} values (0.72× BBG) derived from the sigmoidal regression of inhibition of A11-reactive Aβ species formation by BBG (Figure 6D). Therefore, we conclude that the inhibition of Aβ-associated cytotoxicity directly correlates with BBG aggregation modulation effects. Furthermore, considering that BBG-induced aggregates are nontoxic, Aβ-associated cytotoxicity reduction is attributed to BBG-induced, nontoxic aggregate formation.

Bias of ThT Fluorescence Reading at High Concentration of BBG. We used ThT binding to verify the onset of fibril formation at varying BBG concentrations. As BBG concentration was increased, the ThT fluorescence of Aβ samples decreased accordingly (Figure 5), consistent with our findings and observations at 3× BBG. In order to quantify the inhibition of ThT fluorescence by BBG, we plotted ThT fluorescence versus BBG concentrations from 10^{-5}× to 10× BBG (Supporting Information Figure S3). Data fitting to a sigmoid curve ($R^2 = 0.99$) generated an IC_{50} value of 0.03× BBG, which is 1 order of magnitude lower than those determined for the inhibition of A11-reactive species formation by BBG. To explain this discrepancy, we hypothesized that the ThT fluorescence reading was biased due to either spectral interference of BBG on ThT fluorescence measurement or competitive binding of BBG to ThT binding sites on amyloid fibrils. Carver et al. reported that curcumin and quercetin significantly skewed ThT fluorescence measurements via spectral interference, where alternatively resveratrol introduced a measurement bias by competing with ThT for amyloid fibril binding sites.[82] Since BBG at neutral pH has negligible absorbance at both 450 nm (excitation wavelength of ThT fluorescence) and 485 nm (emission wavelength of ThT fluorescence),[83] spectral interference was ruled out as a source of the bias. Next, to determine whether BBG and ThT competitively bind to the same sites, we measured the ThT fluorescence of preformed amyloid fibrils that were momentarily mixed with varying BBG concentrations immediately prior to adding ThT

(Supporting Information Figure S4). As BBG concentration increased, ThT fluorescence decreased accordingly. When the data were fitted to a sigmoidal curve ($R^2 = 0.99$), an IC_{50} value of 0.16× BBG was obtained. From this, we conclude that the ThT fluorescence measurements of Aβ samples coincubated with BBG can be biased since BBG at high concentrations can interfere with ThT binding to amyloid fibrils. Consequently, the ThT fluorescence assay should be used with caution at high concentrations of BBG.

Comparison of the Aβ Aggregates Formed in the Presence or Absence of BBG. TEM, ThT fluorescence, immunoblotting, and cellular reducing activity assays have demonstrated various differences between the Aβ aggregates formed with BBG and those formed without BBG. In particular, the Aβ aggregates incubated for 2 days with and without 3× BBG exhibited several noticeable differences. The TEM images clearly indicate that 3× BBG inhibits long fibril formation but promotes ∼100 nm long curvilinear protofibril formation (Figure 3 top middle and bottom middle). At day 2, Aβ aggregates formed without BBG exhibited a moderate increase in ThT fluorescence compared to Aβ monomers (Figure 5), which suggests that fibrillar and nonfibrillar aggregates exist together. Unfortunately, the reduction in the ThT fluorescence value of the Aβ aggregates formed with 3× BBG cannot be directly interpreted as an indication of a reduction of Aβ fibrils due to the interference issue. The Aβ aggregates formed with 3× BBG showed very weak A11-reactivity, whereas the Aβ aggregates formed without BBG exhibited a substantial A11-reactivity. The protofibrils (Figure 3 top middle) look similar to the A11-reactive Aβ40 protofibrils that Kim et al. recently reported.[39] In the presence of 3× BBG, the 4G8-reactivity of the Aβ aggregates decreased (Figure 2), which suggests that one of the BBG binding sites might be located to near the 4G8 epitope, the hydrophobic patch of Aβ at the 3× BBG concentration.

At day 2, the Aβ aggregates formed without BBG exhibited a significant decrease in the cellular reducing activity in both MTT (Figure 8) and alamar blue (Supporting Information Figure S2) assays. These two assays indicate the reduced cell viability is correlated with the A11-reactivity (Figure 2). The significantly reduced A11-reactivity of the Aβ aggregates formed with 3× BBG suggests its correlation with the substantial increase in the cellular reducing activity on both MTT (Figure 8) and alamar blue (Supporting Information Figure S2). A11-reactivity is defined by immunoreactivity of Aβ aggregates but not by size or morphology. Therefore, it remains unclear whether there is any correlation between the A11-reactivity and the size or morphology of Aβ aggregates. Considering that the BBG-induced Aβ aggregates do not form Aβ fibrils or at least substantially slow down the fibril formation process, we speculate that BBG binding causes conformation changes of Aβ protofibrils or blocking the nuclei leading to inhibition of fibril formation. However, further investigation is required to clarify the relationship between the BBG-induced Aβ aggregate morphology change and the change in the cellular MTT and alamar blue reducing activity.

Modulation of Aβ Aggregation by BBG Analogues. In order to determine whether any structural features of BBG are critical in modulating Aβ aggregation and cytotoxicity, Aβ aggregation modulation capacity of three close structural analogues of BBG (BBR, BBF, and FGF) were examined using dot-blotting and TEM analysis. The four compounds (BBG, BBR, BBF, and FGF) are congeners sharing the common triphenylmethane structure. Both BBF and FGF are FDA-approved food dyes.[84] Similar to BBG, BBR is commonly used to stain proteins in protein electrophoresis. However, the chemical structure of BBR differs from BBG by the lack of two methyl groups attached to triphenylmethane (Figure 1). Both BBF and FGF have three benzenesulfonate functional groups, whereas BBG and BBR have two benzenesulfonate functional groups and one uncharged diphenylamine group. FGF differs from BBF with only one hydroxyl functional group attached to one of the benzenesulfonate functional groups (Figure 1).

Three different concentrations (1×, 3×, and 10×) of each BBG analogue were coincubated with 50 μM of Aβ for up to 3 days, and the immunoreactivities of the Aβ samples were monitored by A11, 4G8, and 6E10 Aβ-specific antibodies. Similar to BBG, BBR reduced toxic A11-reactive Aβ species. 3× BBR made the A11-reactivity less than half the A11-reactive signal of Aβ sample incubated without any dye, though 1× BBR did not make a substantial change in the A11-reactive signal (Figure 10A). Coincubation of 10× BBR with the Aβ samples led to almost complete elimination of the A11-reactive species. However, considering that even 1× BBG substantially reduced the A11-reactivity (Figure 10A), BBR is less effective than BBG in reducing A11-reactive species. Similar to 10× BBG, 10× BBR substantially reduced the 4G8-reactive signal, suggesting that both BBR and BBG bind to the Aβ hydrophobic patch (4G8 epitope) in a similar fashion (Figure 10B). In contrast, even at 10× BBR, there was no substantial reduction of the 6E10-reactive signal, which suggests that the BBR interaction mode of Aβ is different from that of BBG (Figures 6C and 10C). These results suggest that BBR reduces A11-reactive toxic species, but the interaction mode of BBR with Aβ is different from that of BBG.

In sharp contrast to BBG, both BBF and FGF caused little or no change in the A11- and 4G8-immunoreactivity of the Aβ samples compared to that of the no dye control (Figure 10). In particular, even 10× BBF and 10× FGF did not show any substantial reduction of the neurotoxic A11-reactive Aβ species. At day 3, the Aβ samples incubated with either BBF or FGF exhibited strong 6E10 signals, whereas Aβ aggregates formed in the absence of any dye exhibited very weak 6E10 signals (Figure 10C). These 6E10 epitope accessibility results suggest that BBF- or FGF-induced Aβ protofibrils and fibrils have conformations different from those of Aβ protofibrils and fibrils formed in the absence of any dye.

The morphology of Aβ aggregates formed after 2 days in the absence (no dye control) or presence of one of the BBG congeners was analyzed by negative-stain TEM (Figure 4). Similar to BBG, coincubation of 10× BBR promoted protofibril formation (less than 100 nm), but inhibited amyloid fibril formation (Figure 4B and C). In contrast, both BBF and FGF induced formation of the mixture of long fibrils and protofibrils, whereas the Aβ aggregates incubated with BBG for 2 days were predominantly curvilinear protofibrils (Figure 4B, D, and E). The morphology of the Aβ aggregates formed in the presence of either BBF (Figure 4D) or FGF (Figure 4E) was similar to that of the Aβ aggregates formed in the absence of any dye (Figure 4A), which is consistent with the dot-blot results that there are little or minor differences in the immunoreactivities of the Aβ aggregates formed in the absence or in the presence of BBF or FGF.

These results strongly suggest that both BBG and BBR effectively modulate Aβ aggregation by promoting protofibril formation but inhibiting fibril formation. In contrast, both BBF

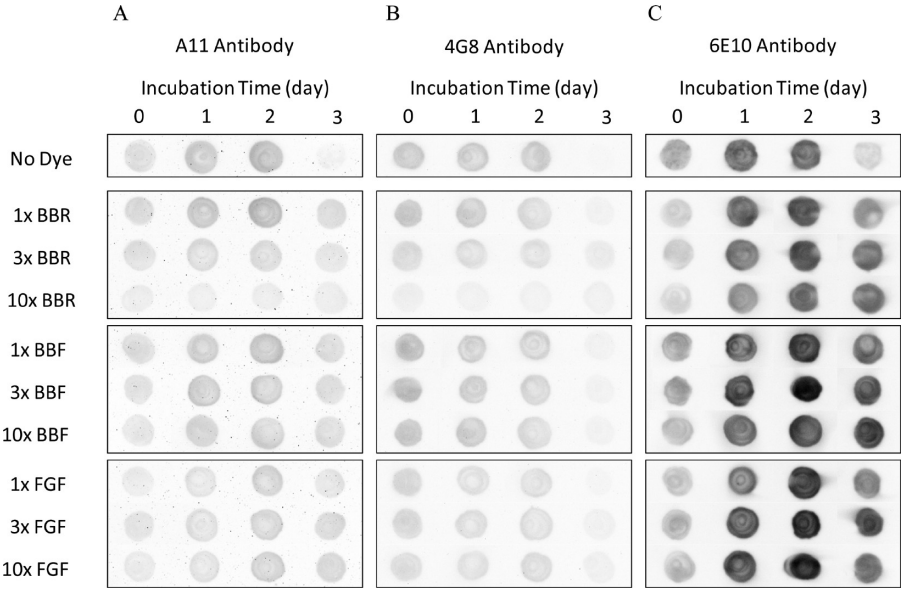

Figure 10. Modulation of Aβ aggregation by BBG analogues, BBR, BBF, and FGF. 50 μM of Aβ monomer was incubated at 37 °C in the absence (no dye) or presence of the indicated concentrations of BBR, BBF, or FGF (1×, 3×, and 10×) for up to 3 days. Samples were taken on the indicated day and spotted onto a nitrocellulose membrane. Each membrane was immunostained with the A11 (A), 4G8 (B), or 6E10 (C) antibody.

and FGF are not as effective in modulating Aβ aggregation as BBG and BBR, but promote formation of the mixture of protofibrils and fibrils.

Modulation of Aβ Cytotoxicity by BBG Analogues. Modulating effects of the BBG analogues on Aβ-associated cytotoxicity were also evaluated by MTT reduction assay of SH-SY5Y cells (Figure 11). Similar to 3× BBG, coincubation of 3× BBR with Aβ samples recovered the viability of SH-SY5Y cells from 76% to 97% (Figure 11), which is consistent with the reduced neurotoxic A11-reactivity of the Aβ aggregates at 3× BBR (Figure 10A). However, compared with 1× BBG, coincubation of 1× BBR exhibits less increase in the SH-SY5Y cell viability (86%) consistent with lower reduction of the A11-reactivity. These findings support the idea that BBR reduces Aβ-associated cytotoxicity but is less effective than BBG.

In contrast, BBF and FGF are less effective in modulating the Aβ-cytotoxicity than BBG and BBR. Even at 3× BBF and FGF, the SH-SY5Y cell viability was 80% and 86%, respectively, which is higher than the cell viability without any dye but 10% lower than the cell viability with either 3× BBG or 3× BBR. A moderate reduction of Aβ cytotoxicity produced by BBF or FGF may be due to promoted formation of less toxic fibrils than oligomers/protofibrils (Figure 4D and E). Investigations are underway to reveal the underlying mechanisms for this behavior.

Based on our findings, we identified several important BBG structural features that are important for modulating Aβ aggregation and cytotoxicity. Although all four triphenylmethane-based BBG and analogues exhibit modulating ability on Aβ aggregation, structural differences of BBG and BBR from BBF and FGF (one additional diphenylamine group and one less benzenesulfonate group) are responsible for the unique interaction mode of BBG and BBR on Aβ leading to formation of nontoxic Aβ aggregates. In particular, one sulfonate group connected to the triphenylmethane backbone contains an electron withdrawing sulfur atom that is expected to perturb $\pi-\pi$ stacking interaction. Furthermore, considering that BBG is more effective in modulating Aβ aggregation and cytotoxicity than BBR, the two additional methyl groups in BBG should also be considered important.

Taken together, our results conclusively establish that BBG effectively reduces neurotoxic A11-reactive Aβ intermediates by inducing the formation of nontoxic Aβ aggregates. BBG inhibited the formation of A11-reactive Aβ aggregates in a dose-dependent manner. The IC_{50} value in the inhibition of A11-reactive Aβ aggregate formation by BBG after 2 day incubation was 0.72× BBG. Negative-stain TEM, ThT fluorescence assay, and dot-blotting assay results strongly support the idea that BBG promotes the formation of A11-unreactive, off-pathway Aβ oligomers and protofibrils, but inhibits the formation of amyloid fibrils. BBG at 15 μM (3× BBG) conferred only a minor cytotoxicity (5%) to neuroblastoma SH-SY5Y cells, which is approximately one-third of the cytotoxicity of 5 μM of Aβ monomer. At 3× BBG, Aβ-associated cytotoxicity was completely suppressed throughout the duration of our study (3 days). BBG effectively inhibits Aβ-associated cytotoxicity in a dose-dependent manner. The EC_{50} value of inhibition of Aβ-associated cytotoxicity by BBG was 0.55× BBG. These results strongly support the idea that the inhibition of Aβ-associated cytotoxicity by BBG directly correlates with the reduction of neurotoxic A11-reactive Aβ aggregates by BBG. Comparative studies of BBG and BBG analogues on modulation of Aβ aggregation and cytotoxicity revealed that one additional diphenylamine group and one less benzenesulfonate group are critical for Aβ aggregation modulation. Furthermore, considering that BBG is more effective in modulating Aβ aggregation and cytotoxicity than BBR, the two additional methyl groups attached to the triphenylmethane structure in BBG are also important.

The inhibitory effects of BBG on Aβ-associated cytotoxicity as well as highly favorable biocompatibility and BBB-permeability make BBG a promising lead compound for future AD therapeutic development.

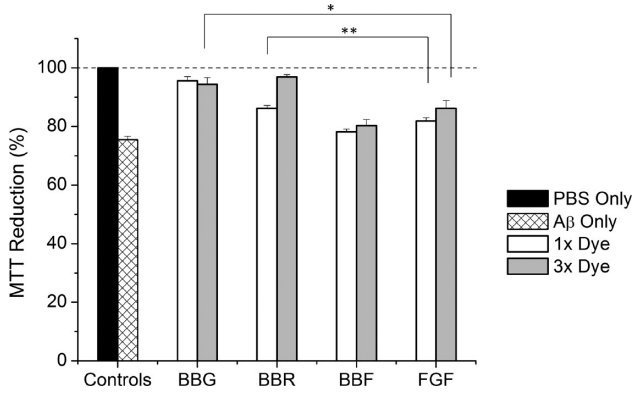

Figure 11. Viability of neuroblastoma SH-SY5Y cells incubated with preformed Aβ samples in the presence of BBG or BBG analogues (BBR, BBF, and FGF). Preformed Aβ aggregates were prepared by incubating 50 μM of Aβ monomer in the presence of BBG or BBG analogues at 37 °C for 2 days, as indicated in the graph. Aggregates were then administered to SH-SY5Y cells at a final concentration of 5 μM. After 48 h, mitochondrial metabolic activity was measured using MTT reduction. Cells administered with PBS as a control (black), Aβ samples incubated without BBG (white with pattern), Aβ samples incubated with 1× dye (white), or 3× dye (gray). Values represent means ± standard deviation ($n \geq 3$). Values are normalized to the viability of cells administered with PBS only. Two-sided Student's t tests were applied to the data. *P < 0.001, **P < 0.01.

METHODS

Materials. Aβ40 was purchased from Anaspec, Inc. (Fremont, CA). Human neuroblastoma SH-SY5Y cells were obtained from the American Type Culture Collection (ATCC; Manassas, VA). Polyclonal A11 anti-oligomer and horseradish peroxidase (HRP)-conjugated anti-rabbit IgG antibodies were obtained from Invitrogen (Carlsbad, CA). 4G8 antibody was obtained from Abcam (Cambridge, MA). Monoclonal 6E10 was obtained from Millipore (Billerica, MA). ECL advance chemiluminescence kit was obtained from GE Healthcare Life Sciences. Alamar blue dye stock solution (10×) was obtained from Invitrogen (Calsbad, CA). All other chemicals were obtained from Sigma-Aldrich (St. Louis, MO) unless otherwise noted.

Aβ Sample Preparation. Aβ40 samples were prepared as described earlier.[59−61] Aβ40 was dissolved in 0.1% triflouroacetic acid (TFA) to obtain a 1.0 mM stock solution, which was then incubated for 1 h at room temperature without agitation. The freshly prepared 1.0 mM stock Aβ40 solution was diluted with phosphate buffered saline (PBS) solution (10 mM NaH_2PO_4 and 150 mM NaCl at pH 7.4) to obtain a 50 μM Aβ solution. Aβ samples of 50 μM were then incubated at 37 °C for the desired time.

Dot-Blotting. Aβ40 samples (2 μL) were spotted onto a nitrocellulose membrane and were allowed to dry at room temperature. The nitrocellulose membrane was incubated in 5% skim milk dissolved in 0.1% Tween 20, Tris-buffered saline (TBS-T) solution for 1 h. The 5% milk TBS-T solution was removed, and the membrane was washed three times for 5 min each with TBS-T solution. The membrane was then incubated in antibody solution for 1 h. The 4G8, A11, and 6E10 antibodies were diluted in 0.5% milk TBS-T solution according to the manufacturer's recommendation. After incubation, the membrane was washed three times for 5 min using TBS-T solution. When a peroxidase (HRP)-conjugated antibody (4G8) was used as the primary antibody, membranes were coated with 2 mL of detection agent from the ECL Advance Detection Kit (GE Healthcare, Waukesha, WI) and the fluorescence was visualized. Otherwise, the membrane was incubated in (1:5000 dilution in 0.5% milk TBS-T) HRP-conjugated IgG for 1 h. Then the membrane was washed three times for 5 min each with TBS-T solution, and the same detection method as previously described was used. The blot images were captured using a BioSpectrum imaging system (UVP, Upland, CA).

ThT Fluorescence Assay. An amount of 5 μL of 50 μM Aβ40 sample solution was diluted in 250 μL of 10 μM ThT (dissolved in PBS) in 96-well plates. The resulting ThT fluorescence of Aβ samples was measured at an emission wavelength of 485 nm using an excitation wavelength of 450 nm using a Synergy 4 UV−vis/fluorescence multimode microplate reader (Biotek, Winooski, VT).

TEM. A 10 μL Aβ sample was adsorbed onto a Formvar mesh grid for 1 min. The grids were then negatively stained with 2% uranyl acetate for 45 s, blotted dry, and viewed on a Jeol JEM1230 transmission electron microscope at the Advanced Microscopy Laboratory at the University of Virginia operated at 80 kV.

Aβ-BBG Binding Assay. A saturation curve of BBG binding to Aβ was obtained according to the Bradford assay protocols described previously.[63,85,86] A 0.05 g/mL stock solution of BBG was prepared by dissolving BBG powder in water. An acidified alcohol solution was prepared by combining 95% ethanol and 85% phosphoric acid in a 1:2 volumetric ratio. Then the modified Bradford reagent was created by adding 167 μL of the BBG stock solution to 250 μL of the acidified alcohol and the final volume was adjusted to 1 mL. For each sample, 50 μL of the modified Bradford reagent was added to each well in a 96-well microplate. Next, 0−30 μL of 1 mM Aβ monomer was added to each well, and the final volume was adjusted to 100 μL with double distilled water. Absorbance of the samples was measured at 595 nm using a Synergy 4 UV−vis/fluorescence multimode microplate reader (Biotek, Winooski, VT). The number of BBG binding sites and the intrinsic binding constant were derived from the saturation binding curve. The detailed procedures are described in the Supporting Information.

MTT and Alamar Blue Reduction Assays. A total of 50 mg of MTT obtained from Millipore (Billerica, MA) was dissolved overnight at 4 °C in 10 mL of PBS. The MTT solution was then sterile filtered. Human neuroblastoma SH-SY5Y cells were cultured in a humidified 5% CO_2/air incubator at 37 °C in DMEM 12:1:1 modified media with 10% fetal bovine serum and 1% penicillin-streptomycin (Thermofisher, Waltham, MA). A total of 25 000 SH-SY5Y cells were seeded into 96-well plates and incubated for 48 h. After incubation, the culture medium was replaced with 100 μL of fresh media, and 10 μL of the Aβ sample was added to each well to obtain a final Aβ concentration of 5 μM. Cells were incubated for an additional 48 h. The media was then aspirated and replaced with 50 μL of fresh media. Then 10 μL of the sterile MTT solution was added, and cells were incubated for 6 h at 37 °C in the dark. After incubation, 200 μL of DMSO was added to each well to dissolve the reduced MTT, and the absorbance was measured at 506 nm using a Synergy 4 UV−vis/fluorescence multimode microplate reader.

Alamar blue reduction assay was performed according to the protocol in the literature [79−81] and the manufacturer's protocol (Invitrogen) with some modifications. A total of 10 000 SH-SY5Y cells were seeded at each well in a 96-well plate. The cells were incubated for up to 1 week. After incubation, old media were replaced with 100 μL of fresh media, and 10 μL of the sample containing Aβ with or without BBG was added to each well. The cells were incubated for 3 days, and the media was then replaced with 100 μL of fresh media followed by addition of 40 μL of a 10× alamar blue stock solution. Next, the cells were incubated for 4−6 h to allow the cells to metabolize the alamar blue. After incubation, fluorescence was measured using an emission wavelength of 590 nm using an excitation wavelength of 555 nm using a Synergy 4 UV−vis/fluorescence microplate reader (Biotek, Winooski, VT).

■ ASSOCIATED CONTENT

Supporting Information. Figure S1 showing the BBG-Aβ binding curve data fitted into a straight-line. Figure S2 showing the alamar blue reducing activities of cells treated with Aβ samples incubated without BBG for 0 to 3 days or with 3× BBG for 2 days. Figure S3 showing the dose-dependence of inhibition of ThT fluorescence of Aβ samples by BBG. Figure S4 showing ThT fluorescence of preformed amyloid fibrils (72 h) mixed with varying concentrations of BBG immediately prior to addition of ThT. This material is available free of charge via the Internet at http://pubs.acs.org.

■ AUTHOR INFORMATION

Corresponding Author

*E-mail: ik4t@virginia.edu. Telephone: 434-243-1822. Fax: 434-982-2658.

Author Contributions

H.E.W. performed the experimental work, data analysis, and manuscript writing and preparation. W.Q. developed methods. H.-M.C. and E.J.F. provided guidance and advice. I.K. provided guidance and advice and also performed data analysis and manuscript writing and preparation.

Funding Sources

This work was supported by the School of Engineering and Applied Science, University of Virginia and a KSEA Young Investigator Grant (I.K.).

■ ACKNOWLEDGMENT

We thank Dr. Jan Redick and Dr. Stacey Guillot of the Advanced Microscopy Laboratory at the University of Virginia for their assistance with Aβ sample TEM assays. We are grateful to Dr. Theresa Good of the University of Maryland at Baltimore County for discussion and valuable comments on Aβ sample preparation and Aβ-associated cytotoxicity assay.

■ ABBREVIATIONS

AD, Alzheimer's disease; Aβ, amyloid-beta; BBG, Brilliant Blue G; BBF, Brilliant Blue FCF; BBR, Brilliant Blue R; ThT, Thioflavin T; DMSO, dimethyl sulfoxide; EC_{50}, half-maximal enhancement value; FDA, U.S. Food and Drug Administration; HRP, horseradish peroxidase; IC_{50}, half-maximal inhibitory value; MTT, 3-(4,5-dimethylthiazol-2-yl)-2,5-diphenyltetrazolium bromide; PBS, phosphate-buffered saline; TBS, Tris-buffered saline; TBS-T, 0.1% Tween 20 in Tris-buffered saline; TEM, transmission electron microscopy

■ REFERENCES

(1) Brookmeyer, R., Gray, S., and Kawas, C. (1998) Projections of Alzheimer's disease in the United States and the public health impact of delaying disease onset. *Am. J. Public Health 88*, 1337–1342.

(2) Alzheimer's Association. (2010) 2010 Alzheimer's disease facts and figures. *Alzheimer's Dementia 6*, 158−194.

(3) Sinha, S., and Lieberburg, I. (1999) Cellular mechanisms of beta-amyloid production and secretion. *Proc. Natl. Acad. Sci. U.S.A. 96*, 11049–11053.

(4) Bitan, G., Kirkitadze, M. D., Lomakin, A., Vollers, S. S., Benedek, G. B., and Teplow, D. B. (2003) Amyloid beta-protein (Aβ) assembly: Aβ40 and Aβ42 oligomerize through distinct pathways. *Proc. Natl. Acad. Sci. U.S.A. 100*, 330–335.

(5) Hardy, J. A., and Higgins, G. A. (1992) Alzheimers disease - the amyloid cascade hypothesis. *Science 256*, 184–185.

(6) Hardy, J., and Selkoe, D. J. (2002) Medicine - The amyloid hypothesis of Alzheimer's disease: Progress and problems on the road to therapeutics. *Science 297*, 353–356.

(7) McLean, C. A., Cherny, R. A., Fraser, F. W., Fuller, S. J., Smith, M. J., Beyreuther, K., Bush, A. I., and Masters, C. L. (1999) Soluble pool of Aβ amyloid as a determinant of severity of neurodegeneration in Alzheimer's disease. *Ann. Neurol. 46*, 860–866.

(8) Ladiwala, A. R. A., Lin, J. C., Bale, S. S., Marcelino-Cruz, A. M., Bhattacharya, M., Dordick, J. S., and Tessier, P. M. (2010) Resveratrol selectively remodels soluble oligomers and fibrils of amyloid Aβ into off-pathway conformers. *J. Biol. Chem. 285*, 24228–24237.

(9) Chimon, S., Shaibat, M. A., Jones, C. R., Calero, D. C., Aizezi, B., and Ishii, Y. (2007) Evidence of fibril-like β-sheet structures in a neurotoxic amyloid intermediate of Alzheimer's β-amyloid. *Nat. Struct. Mol. Biol. 14*, 1157–1164.

(10) Hawkes, C. A., Ng, V., and McLaurin, J. (2009) Small molecule inhibitors of Aβ-aggregation and neurotoxicity. *Drug Dev. Res. 70*, 111–124.

(11) Hamaguchi, T., Ono, K., and Yamada, M. (2006) Anti-amyloidogenic therapies: strategies for prevention and treatment of Alzheimer's disease. *Cell. Mol. Life Sci. 63*, 1538–1552.

(12) Thapa, A., Woo, E. R., Chi, E. Y., Sharoar, M. G., Jin, H. G., Shin, S. Y., and Park, I. S. (2011) Biflavonoids are superior to monoflavonoids in inhibiting amyloid-β toxicity and fibrillogenesis via accumulation of nontoxic oligomer-like structures. *Biochemistry 50*, 2445–2455.

(13) Necula, M., Kayed, R., Milton, S., and Glabe, C. G. (2007) Small molecule inhibitors of aggregation indicate that amyloid β oligomerization and fibrillization pathways are independent and distinct. *J. Biol. Chem. 282*, 10311–10324.

(14) Bose, P. P., Chatterjee, U., Xie, L., Johansson, J., Gothelid, E., and Arvidsson, P. I. (2010) Effects of Congo Red on Aβ(1−40) Fibril formation process and morphology. *ACS Chem. Neurosci. 1*, 315–324.

(15) Burgevin, M. C., Daniel, N., Passat, M., Messence, K., Bertrand, P., Doble, A., and Blanchard, J. C. (1994) Neurotoxicity of beta-amyloid analog peptides on rat hippocampal neuronal cultures. *J. Neurochem. 63*, S74–S74.

(16) Lorenzo, A., and Yankner, B. A. (1994) β-Amyloid neurotoxicity requires fibril formation and is inhibited by congo red. *Proc. Natl. Acad. Sci. U. S. A. 91*, 12243–12247.

(17) Pedersen, M. O., Mikkelsen, K., Behrens, M. A., Pedersen, J. S., Enghild, J. J., Skrydstrup, T., Malmendal, A., and Nielsen, N. C. (2010) NMR reveals two-step association of congo red to amyloid β in low-molecular-weight aggregates. *J. Phys. Chem. B 114*, 16003–16010.

(18) Podlisny, M. B., Walsh, D. M., Amarante, P., Ostaszewski, B. L., Stimson, E. R., Maggio, J. E., Teplow, D. B., and Selkoe, D. J. (1998) Oligomerization of endogenous and synthetic amyloid β-protein at nanomolar levels in cell culture and stabilization of monomer by congo red. *Biochemistry 37*, 3602–3611.

(19) McLaurin, J., Golomb, R., Jurewicz, A., Antel, J. P., and Fraser, P. E. (2000) Inositol stereoisomers stabilize an oligomeric aggregate of Alzheimer amyloid beta peptide and inhibit A β-induced toxicity. *J. Biol. Chem. 275*, 18495–18502.

(20) McLaurin, J., Kierstead, M. E., Brown, M. E., Hawkes, C. A., Lambermon, M. H. L., Phinney, A. L., Darabie, A. A., Cousins, J. E., French, J. E., Lan, M. F., Chen, F. S., Wong, S. S. N., Mount, H. T. J., Fraser, P. E., Westaway, D., and St George-Hyslop, P. (2006) Cyclohexanehexol inhibitors of Aβ aggregation prevent and reverse Alzheimer phenotype in a mouse model. *Nat. Med. 12*, 801–808.

(21) Ehrnhoefer, D. E., Bieschke, J., Boeddrich, A., Herbst, M., Masino, L., Lurz, R., Engemann, S., Pastore, A., and Wanker, E. E. (2008) EGCG redirects amyloidogenic polypeptides into unstructured, off-pathway oligomers. *Nat. Struct. Mol. Biol. 15*, 558–566.

(22) Feng, Y., Wang, X.-P., Yang, S.-G., Wang, Y.-J., Zhang, X., Du, X.-T., Sun, X.-X., Zhao, M., Huang, L., and Liu, R.-T. (2009) Resveratrol inhibits beta-amyloid oligomeric cytotoxicity but does not prevent oligomer formation. *Neurotoxicology 30*, 986–995.

(23) Reinke, A. A., and Gestwicki, J. E. (2007) Structure-activity relationships of amyloid beta-aggregation inhibitors based on curcumin: Influence of linker length and flexibility. *Chem. Biol. Drug Des. 70*, 206–215.

(24) Yang, F. S., Lim, G. P., Begum, A. N., Ubeda, O. J., Simmons, M. R., Ambegaokar, S. S., Chen, P. P., Kayed, R., Glabe, C. G., Frautschy, S. A., and Cole, G. M. (2005) Curcumin inhibits formation of amyloid β oligomers and fibrils, binds plaques, and reduces amyloid in vivo. *J. Biol. Chem. 280*, 5892–5901.

(25) Moss, M. A., Varvel, N. H., Nichols, M. R., Reed, D. K., and Rosenberry, T. L. (2004) Nordihydroguaiaretic acid does not disaggregate β-amyloid(1−40) protofibrils but does inhibit growth arising from direct protofibril association. *Mol. Pharmacol. 66*, 592–600.

(26) Pardridge, W. A. (2009) Alzheimer's disease drug development and the problem of the blood-brain barrier. *Alzheimer's Dementia 5*, 427–432.

(27) Frid, P., Anisimov, S. V., and Popovic, N. (2007) Congo red and protein aggregation in neurodegenerative diseases. *Brain Res. Rev. 53*, 135–160.

(28) Ladiwala, A. R. A., Dordick, J. S., and Tessier, P. M. (2010) Aromatic small molecules remodel toxic soluble oligomers of amyloid β through three independent pathways. *J. Biol. Chem. 286*, 3209–3218.

(29) Zini, A., Del Rio, D., Stewart, A. J., Mandrioli, J., Merelli, E., Sola, P., Nichelli, P., Serafini, M., Brighenti, F., Edwards, C. A., and Crozier, A. (2006) Do flavan-3-ols from green tea reach the human brain? *Nutr. Neurosci. 9*, 57–61.

(30) Yazawa, K., Kihara, T., Shen, H. L., Shimmyo, Y., Niidome, T., and Sugimoto, H. (2006) Distinct mechanisms underlie distinct polyphenol-induced neuroprotection. *FEBS Lett. 580*, 6623–6628.

(31) Diniz, A., Escuder-Gilabert, L., Lopes, N. P., Gobbo-Neto, L., Villanueva-Camanas, R. M., Sagrado, S., and Medina-Hernandez, M. J. (2007) Permeability profile estimation of flavonoids and other phenolic compounds by biopartitioning micellar capillary chromatography. *J. Agric. Food Chem. 55*, 8372–8379.

(32) Remy, M., Thaler, S., Schumann, R. G., May, C. A., Fiedorowicz, M., Schuettauf, F., Gruterich, M., Priglinger, S. G., Nentwich, M. M., Kampik, A., and Haritoglou, C. (2008) An in vivo evaluation of Brilliant Blue G in animals and humans. *Br. J. Ophthalmol. 92*, 1142–1147.

(33) Peng, W. G., Cotrina, M. L., Han, X. N., Yu, H. M., Bekar, L., Blum, L., Takano, T., Tian, G. F., Goldman, S. A., and Nedergaard, M. (2009) Systemic administration of an antagonist of the ATP-sensitive receptor P2 × 7 improves recovery after spinal cord injury. *Proc. Natl. Acad. Sci. U.S.A. 106*, 12489–12493.

(34) Borzelleca, J. F., Depukat, K., and Hallagan, J. B. (1990) Lifetime toxicity carcinogenicity studies of FD&C blue No.1 (brilliant blue FCF) in rats and mice. *Food Chem. Toxicol. 28*, 221–234.

(35) Borzelleca, J. F., and Hallagan John, B. (1992) Safety and Regulatory Status of Food, Drug, and Cosmetic Color Additives. In *Food Safety Assessment* (Finley, J. W., Robinson, S. F., and Armstrong, D. J., Eds.), pp 377−390, American Chemical Society, Washington, D.C.

(36) Ryu, J. K., and McLarnon, J. G. (2008) Block of purinergic P2X(7) receptor is neuroprotective in an animal model of Alzheimer's disease. *NeuroReport 19*, 1715–1719.

(37) Matute, C., Torre, I., Perez-Cerda, F., Perez-Samartin, A., Alberdi, E., Etxebarria, E., Arranz, A. M., Ravid, R., Rodriguez-Antiguedad, A., Saanchez-Goomez, M. V., and Domercq, M. (2007) P2X(7) receptor blockade prevents ATP excitotoxicity in oligodendrocytes and ameliorates experimental autoimmune encephalomyelitis. *J. Neurosci. 27* 9525–9533.

(38) Kayed, R., Head, E., Thompson, J. L., McIntire, T. M., Milton, S. C., Cotman, C. W., and Glabe, C. G. (2003) Common structure of soluble amyloid oligomers implies common mechanism of pathogenesis. *Science 300*, 486–489.

(39) Hu, Y., Su, B. H., Kim, C. S., Hernandez, M., Rostagno, A., Ghiso, J., and Kim, J. R. (2010) A strategy for designing a peptide probe for detection of β-amyloid oligomers. *ChemBioChem 11*, 2409–2418.

(40) Khurana, R., Coleman, C., Ionescu-Zanetti, C., Carter, S. A., Krishna, V., Grover, R. K., Roy, R., and Singh, S. (2005) Mechanism of thioflavin T binding to amyloid fibrils. *J. Struct. Biol. 151*, 229–238.

(41) LeVine, H. (1999) Quantification of β-sheet amyloid fibril structures with thioflavin T. In *Methods in Enzymology* 309 (Ronal, W., Ed.), pp 274−284, Academic Press, New York.

(42) Dahlgren, K. N., Manelli, A. M., Stine, W. B., Baker, L. K., Krafft, G. A., and LaDu, M. J. (2002) Oligomeric and fibrillar species of amyloid-β peptides differentially affect neuronal viability. *J. Biol. Chem. 277*, 32046–32053.

(43) Shafrir, Y., Durell, S. R., Anishkin, A., and Guy, H. R. (2010) Beta-barrel models of soluble amyloid beta oligomers and annular protofibrils. *Proteins 78*, 3458–3472.

(44) Chen, Y. R., and Glabe, C. G. (2006) Distinct early folding and aggregation properties of Alzheimer amyloid-β peptides Aβ40 and Aβ42 - Stable trimer or tetramer formation by A beta 42. *J. Biol. Chem. 281*, 24414–24422.

(45) Kayed, R., Head, E., Sarsoza, F., Saing, T., Cotman, C. W., Necula, M., Margol, L., Wu, J., Breydo, L., Thompson, J. L., Rasool, S., Gurlo, T., Butler, P., and Glabe, C. G. (2007) Fibril specific, conformation dependent antibodies recognize a generic epitope common to amyloid fibrils and fibrillar oligomers that is absent in prefibrillar oligomers. *Mol. Neurodegener. 2*, 18.

(46) Wu, J. W., Breydo, L., Isas, J. M., Lee, J., Kuznetsov, Y. G., Langen, R., and Glabe, C. (2010) Fibrillar oligomers nucleate the oligomerization of monomeric amyloid β but do not seed fibril formation. *J. Biol. Chem. 285*, 6071–6079.

(47) Iijima, K., Liu, H. P., Chiang, A. S., Hearn, S. A., Konsolaki, M., and Zhong, Y. (2004) Dissecting the pathological effects of human Aβ40 and Aβ42 in Drosophila: A potential model for Alzheimer's disease. *Proc. Natl. Acad. Sci. U.S.A. 101*, 6623–6628.

(48) Kimura, N., Yanagisawa, K., Terao, K., Ono, F., Sakakibara, I., Ishii, Y., Kyuwa, S., and Yoshikawa, Y. (2005) Age-related changes of intracellular Aβ in cynomolgus monkey brains. *Neuropathol. Appl. Neurobiol. 31*, 170–180.

(49) Klyubin, I., Walsh, D. M., Lemere, C. A., Cullen, W. K., Shankar, G. M., Betts, V., Spooner, E. T., Jiang, L. Y., Anwyl, R., Selkoe, D. J., and Rowan, M. J. (2005) Amyloid β protein immunotherapy neutralizes Aβ oligomers that disrupt synaptic plasticity in vivo. *Nat. Med. 11*, 556–561.

(50) Thakker, D. R., Weatherspoon, M. R., Harrison, J., Keene, T. E., Lane, D. S., Kaemmerer, W. F., Stewart, G. R., and Shafer, L. L. (2009) Intracerebroventricular amyloid-β antibodies reduce cerebral amyloid angiopathy and associated micro-hemorrhages in aged Tg2576 mice. *Proc. Natl. Acad. Sci. U.S.A. 106*, 4501–4506.

(51) Sarroukh, R., Cerf, E., Derclaye, S., Dufrêne, Y., Goormaghtigh, E., Ruysschaert, J.-M., and Raussens, V. (2010) Transformation of amyloid β(1−40) oligomers into fibrils is characterized by a major change in secondary structure. *Cell. Mol. Life Sci.* 1–10.

(52) Mamikonyan, G., Necula, M., Mkrtichyan, M., Ghochikyan, A., Petrushina, I., Movsesyan, N., Mina, E., Kiyatkin, A., Glabe, C. G., Cribbs, D. H., and Agadjanyan, M. G. (2007) Anti-Aβ(1−11) antibody binds to different β-amyloid species, inhibits fibril formation, and disaggregates preformed fibrils but not the most toxic oligomers. *J. Biol. Chem. 282*, 22376–22386.

(53) Schmidt, M., Sachse, C., Richter, W., Xu, C., Fandrich, M., and Grigorieff, N. (2009) Comparison of Alzheimer Aβ(1−40) and Aβ(1−42) amyloid fibrils reveals similar protofilament structures. *Proc. Natl. Acad. Sci. U.S.A. 106*, 19813–19818.

(54) Findeis, M. A. (2000) Approaches to discovery and characterization of inhibitors of amyloid β-peptide polymerization. *Biochim. Biophys. Acta, Mol. Basis Dis. 1502*, 76–84.

(55) Findeis, M. A., and Molineaux, S. M. (1999) Design and testing of inhibitors of fibril formation. In *Methods in Enzymology* 309 (Ronal, W., Ed.), pp 476−488, Academic Press, New York.

(56) Morinaga, A., Ono, K., Takasaki, J., Ikeda, T., Hirohata, M., and Yamada, M. (2011) Effects of sex hormones on Alzheimer's disease-associated β-amyloid oligomer formation in vitro. *Exp. Neurol. 228*, 298–302.

(57) Ono, K., Condron, M. M., Ho, L., Wang, J., Zhao, W., Pasinetti, G. M., and Teplow, D. B. (2008) Effects of grape seed-derived polyphenols on amyloid β-protein self-assembly and cytotoxicity. *J. Biol. Chem. 283*, 32176–32187.

(58) Geng, J., Li, M., Ren, J., Wang, E., and Qu, X. (2011) Polyoxometalates as inhibitors of the aggregation of amyloid beta-peptides associated with Alzheimer's disease. *Angew. Chem., Int. Ed. 18*, 4184–4188.

(59) Qi, W., Zhang, A., Patel, D., Lee, S., Harrington, J. L., Zhao, L. M., Schaefer, D., Good, T. A., and Fernandez, E. J. (2008) Simultaneous monitoring of peptide aggregate distributions, structure, and kinetics using amide hydrogen exchange: Application to Aβ(1−40) fibrillogenesis. *Biotechnol. Bioeng. 100*, 1214–1227.

(60) Qi, W., Zhang, A. M., Good, T. A., and Fernandez, E. J. (2009) Two disaccharides and trimethylamine N-oxide affect Aβ aggregation differently, but all attenuate oligomer-induced membrane permeability. *Biochemistry 48*, 8908–8919.

(61) Zhang, A., Qi, W., Good, T. A., and Fernandez, E. J. (2009) Structural differences between Aβ(1−40) intermediate oligomers and fibrils elucidated by proteolytic fragmentation and hydrogen/deuterium exchange. *Biophys. J. 96*, 1091–1104.

(62) Sandberg, A., Luheshi, L. M., Sollvander, S., de Barros, T. P., Macao, B., Knowles, T. P. J., Biverstal, H., Lendel, C., Ekholm-Petterson, F., Dubnovitsky, A., Lannfelt, L., Dobson, C. M., and Hard, T. (2010) Stabilization of neurotoxic Alzheimer amyloid-β oligomers by protein engineering. *Proc. Natl. Acad. Sci. U.S.A. 107*, 15595–15600.

(63) Sohl, J. L., and Splittgerber, A. G. (1991) The binding of Coomassie brilliant blue to Bovine Serum Albumin: A physical biochemistry experiment. *J. Chem. Educ. 68*, 262–null.

(64) Feng, Y., Yang, S. G., Du, X. T., Zhang, X., Sun, X. X., Zhao, M., Sun, G. Y., and Liu, R. T. (2009) Ellagic acid promotes Aβ42 fibrillization and inhibits Aβ42-induced neurotoxicity. *Biochem. Biophys. Res. Commun. 390*, 1250–1254.

(65) Pollack, S. J., Sadler, I. I. J., Hawtin, S. R., Tailor, V. J., and Shearman, M. S. (1995) Sulfonated dyes attenuate the toxic effects of β-amyloid in a structure-specific fashion. *Neurosci. Lett. 197*, 211–214.

(66) Avramovich-Tirosh, Y., Amit, T., Bar-Am, O., Zheng, H., Fridkin, M., and Youdim, M. B. (2007) Therapeutic targets and potential of the novel brain- permeable multifunctional iron chelator-monoamine oxidase inhibitor drug, M-30, for the treatment of Alzheimer's disease. *J. Neurochem. 100*, 490–502.

(67) Avramovich-Tirosh, Y., Reznichenko, L., Mit, T., Zheng, H., Fridkin, M., Weinreb, O., Mandel, S., and Youdim, M. B. (2007) Neurorescue activity, APP regulation and amyloid-β peptide reduction by novel multi-functional brain permeable iron- chelating- antioxidants, M-30 and green tea polyphenol, EGCG. *Curr. Alzheimer Res. 4*, 403–411.

(68) Lee, S., Fernandez, E. J., and Good, T. A. (2007) Role of aggregation conditions in structure, stability, and toxicity of intermediates in the Aβ fibril formation pathway. *Protein Sci. 16*, 723–732.

(69) Reznichenko, L., Amit, T., Zheng, H., Avramovich-Tirosh, Y., Youdim, M. B., Weinreb, O., and Mandel, S. (2006) Reduction of iron-regulated amyloid precursor protein and β-amyloid peptide by (-)-epigallocatechin-3-gallate in cell cultures: implications for iron chelation in Alzheimer's disease. *J. Neurochem. 97*, 527–536.

(70) Ward, R. V., Jennigs, K. H., Jepras, R., Neville, W., Owen, D. E., Hawkins, J., Christie, G., Davis, J. B., George, A. J., Karran, E. H., and Howlett, D. R. (2000) Fractionation and characterization of oligomeric, protofibrillar and fibrillar forms of β-amyloid peptide. *Biochem. J. 348*, 137–144.

(71) Datki, Z., Juhász, A., Gálfi, M., Soós, K., Papp, R., Zádori, D., and Penke, B. (2003) Method for measuring neurotoxicity of aggregating polypeptides with the MTT assay on differentiated neuroblastoma cells. *Brain Res. Bull. 62*, 223–229.

(72) Nishimura, S., Murasugi, T., Kubo, T., Kaneko, I., Meguro, M., Marumoto, S., Kogen, H., Koyama, K., Oda, T., and Nakagami, Y. (2003) RS-4252 inhibits amyloid β-induced cytotoxicity in HeLa cells. *Pharmacol. Toxicol. 93*, 29–32.

(73) Olivieri, G., Otten, U., Meier, F., Baysang, G., Dimitriades-Schmutz, B., Müller-Spahn, F., and Savaskan, E. (2003) β-amyloid modulates tyrosine kinase B receptor expression in SHSY5Y neuroblastoma cells: influence of the antioxidant melatonin. *Neuroscience 120*, 659–665.

(74) Ono, K., Yoshiike, Y., Takashima, A., Hasegawa, K., Naiki, H., and Yamada, M. (2003) Potent anti-amyloidogenic and fibril-destabilizing effects of polyphenols in vitro: implications for the prevention and therapeutics of Alzheimer's disease. *J. Neurochem. 87*, 172–181.

(75) Wang, S. S.-S., Rymer, D. L., and Good, T. A. (2001) Reduction in cholesterol and sialic acid content protects cells from the toxic effects of β-amyloid peptides. *J. Biol. Chem. 276*, 42027–42034.

(76) Liu, Y., and Schubert, D. (1997) Cytotoxic amyloid peptides inhibit cellular 3-(4,5-dimethylthiazol-2-yl)-2,5-diphenyltetrazolium bromide (MTT) reduction by enhancing MTT formazan exocytosis. *J. Neurochem. 69*, 2285–2293.

(77) Abe, K., and Saito, H. (1998) Amyloid β protein inhibits cellular MTT reduction not by suppression of mitochondrial succinate dehydrogenase but by acceleration of MTT formazan exocytosis in cultured rat cortical astrocytes. *Neurosci. Res. 31*, 295–305.

(78) Hertel, C., Hauser, N., Schubenel, R., Seilheimer, B., and Kemp, J. A. (1996) β-Amyloid-induced cell toxicity: Enhancement of 3-(4,5-dimethylthiazol-2-yl)-2,5-diphenyltetrazolium bromide-dependent cell death. *J. Neurochem. 67*, 272–276.

(79) Estus, S., Tucker, H. M., van Rooyen, C., Wright, S., Brigham, E. F., Wogulis, M., and Rydel, R. E. (1997) Aggregated amyloid-β protein induces cortical neuronal apoptosis and concomitant "aptoptotic" pattern of gene induction. *J. Neurosci. 17*, 7736–7745.

(80) Lindhagen-Persson, M., Brännström, K., Vestling, M., Steinitz, M., and Olofsson, A. (2010) Amyloid-β oligomer specificity mediated by the IgM isotype−Implications for a specific protective mechanism exerted by endogenous auto-antibodies. *PLoS One 5*, e13928.

(81) McLaurin, J., Cecal, R., Kierstead, M. E., Tian, X., Phinney, A. L., Manea, M., French, J. E., Lambermon, M. H. L., Darabie, A. A., Brown, M. E., Janus, C., Chishti, M. A., Horne, P., Westaway, D., Fraser, P. E., Mount, H. T. J., Przybylski, M., and St George-Hyslop, P. (2002) Therapeutically effective antibodies against amyloid β peptide target amyloid β residues 4−10 and inhibit cytotoxicity and fibrillogenesis. *Nat. Med. 8*, 1263–1269.

(82) Hudson, S. A., Ecroyd, H., Kee, T. W., and Carver, J. A. (2009) The thioflavin T fluorescence assay for amyloid fibril detection can be biased by the presence of exogenous compounds. *FEBS J. 276*, 5960–5972.

(83) Georgiou, C. D., Grintzalis, K., Zervoudakis, G., and Papapostolou, I. (2008) Mechanism of Coomassie brilliant blue G-250 binding to proteins: a hydrophobic assay for nanogram quantities of proteins. *Anal. Bioanal. Chem. 391*, 391–403.

(84) Hansen, W. H., Long, E. L., Davis, K. J., Nelson, A. A., and Fitzhugh, O. G. (1966) Chronic toxicity of three food colourings: Guinea Green B, Light Green SF Yellowish and Fast Green FCF in rats, dogs and mice. *Food Cosmet. Toxicol. 4*, 389–410.

(85) Bradford, M. M. (1976) Rapid and sensitive method for quantitation of microgram quantifies of protein utilizing principle of protein-dye binding. *Anal. Biochem. 72*, 248–254.

(86) Congdon, R. W., Muth, G. W., and Splittgerber, A. G. (1993) The Binding Interaction of Coomassie Blue with Proteins. *Anal. Biochem. 213*, 407–413.